

Corrosion behavior of HVOF Inconel 625 coating in the simulated marine environment

Peng Chao¹, Zhong Fengping^{1,2,3}, Yuan Meng^{1,2,3}, Xie Shijie¹, Wang Xuebin^{1,2}

彭超, 钟丰平, 袁梦, 谢世杰, 王学斌

1. National Quality Inspection and Testing Center of Special Metal Structural Materials,

Zhejiang Academy of Special Equipment Science, Hangzhou 310020, China;

2. Key Laboratory of Special Equipment Safety Testing Technology of Zhejiang Province, Hangzhou 310020, China;

3. Zhejiang-Ukraine Joint Laboratory for Materials and Welding Testing Technology, Hangzhou 310020, China

Received 18 October 2023; accepted 14 November 2023

Abstract High velocity oxygen fuel (HVOF) spraying process is commonly used to produce superalloy coatings. Inconel 625 coating was prepared on Q235B low carbon steel by HVOF. A series of experiments were conducted to examine the surface and corrosion resistance properties of Inconel 625 HVOF coating. In this paper, potentiodynamic polarization tests and electrochemical impedance spectroscopy (EIS) tests were carried out to evaluate the corrosion resistance of Inconel 625 coating under simulated marine environment. The experimental results showed that Inconel 625 coating revealed low porosity and desired coating thickness. Shift in the corrosion potential (E_{corr}) towards the noble direction combined with much low corrosion current density (i_{corr}) indicating a significant improvement of HVOF Inconel 625 coating compared with the substrate.

Key words high velocity oxygen fuel (HVOF), Inconel 625 coating, marine environment, corrosion

0 Introduction

Seawater is one of the most aggressive and complex corrosion media. The presence of Cl^- , temperature change, erosion and biofouling in marine environment cause rapid and severe corrosion. Corrosion is a big threat to the safety of in coastal and offshore facilities, and also increases economic cost^[1-2]. Low carbon steel exhibits excellent mechanical properties, flexible and desired cost performance^[3-5]. Therefore, it's always selected for manufacturing components in marine industry. However, considering the corrosion problem of materials, an alternative material or a surface modification method are required for material protection in marine environment.

Inconel 625 nickel based alloy has high strength, and excellent anti-fatigue, anti-creep and anti-corrosion performance. It is one of the advanced materials widely used in extreme environments^[6-9]. Therefore, Inconel 625 is considered to use in some coastal and offshore facilities as a barrier for strong corrosion, and strong erosion. It is obviously unrealistic to change the materials completely. Also, Inconel 625 nickel based alloy as a high-temperature alloy is extremely expensive. If nickel based alloy was used as a whole, the cost of facilities would be far beyond the manufacturer's acceptable range^[10-12]. Therefore, using HVOF spraying technique to produce Inconel 625 coating as a protective layer is the alternative solutions. HVOF is the process in which powder is fed into the supersonic flame flow

Foundation item: This work was supported by Zhejiang Provincial Natural Science Foundation of China (No. LTGC23E010001), the Youth Science and Technology Project of Zhejiang Provincial Administration for Market Regulation (No. QN2023427), and Science and Technology Project of State Administration for Market Regulation (No.2022MK054).

Corresponding author: Yuan Meng (1989–), Ph.D., Senior Engineer. Mainly engaged in performance characterization, failure mechanism, and life evaluation of material surface coatings under service conditions. E-mail: yuanmeng@zjtj.org

doi: 10.12073/j.cw.20231018014

of a thermal spraying heat source to achieve the heating and acceleration of powder particles and the deposition of coatings. Because of the extremely high speed of the flame flow, spray particles can be accelerated to ultrasonic speed and be heated to molten or semi molten state. Thereby HVOF can obtain a high-quality coating with high bonding strength and density^[13]. The characteristics of supersonic flame spraying include high bonding strength of the coating, low porosity, no through-hole, no deformation of the work-piece and so on. And it can customize the performance of the coating by modifying process parameters to meet the specific needs of different use scenarios^[11]. Yang et al.^[13] used HVOF technique to prepare NiCr-Cr₃C₂ and Inconel 625 coatings, and conducted high-temperature erosion and molten salt corrosion tests, verifying the feasibility of their application in waste incineration waste heat boilers.

In order to demonstrate the feasibility and effectiveness of HVOF in preventing corrosion in marine environments, this paper describes a recent investigation of the corrosion resistance properties of Inconel 625 alloy (by HVOF) applied on the Q235B low carbon steel substrate in a chlorine-containing environment (3.5 wt. % aqueous NaCl at room

temperature).

1 Experimental

1.1 Sample preparation

Q235B steel was selected as the substrate for this research. The composition of Q235B was listed in Table 1, with a size of $\phi 50$ mm \times 6 mm. Before spraying, 240, 500, 1 000, 1 200 mesh SiC sandpapers was used to grind the surface of the substrate to remove the surface oxide layer. And the grinded surface was cleaned with acetone to remove surface oil stains, and dried in air. The aerosol spherical Inconel 625 powder was applied as the spraying powder, with a particle size range of 15–45 μ m. The main chemical compositions were shown in Table 2. The HVOF spraying equipment was XY-8000M HVOF (Shanghai Xinye Meike New Material Technology Co., Ltd., Shanghai, China). The spraying process parameters were listed in Table 3, and the final coating thickness was set to be about 500 μ m. Subsequently, HVOF Inconel 625 coating was used as the research object, and Q235B substrate was set as the reference sample.

Table 1 Chemical compositions of Q235B steel (wt.%)

C	Si	Mn	P	S	Fe
0.090	0.22	0.40	0.012	0.009 8	Balance

Table 2 Chemical compositions of Inconel 625 powder (wt.%)

Cr	Mo	Fe	Al	Ti	Si	Nb	Ni
21.50	7.41	3.02	0.001	0.006	1.34	3.95	Balance

Table 3 Process Parameters of HVOF

Fuel flow rate/(L·h ⁻¹)	O ₂ flow rate/(m ³ ·h ⁻¹)	powder feed rate/(g·min ⁻¹)	Carrier gas flow rate/(L·min ⁻¹)	Spray distance/mm	Chamber pressure/MPa
25	66	45 – 50	0.75	350	6.88

1.2 Electrochemical testing

Potentiodynamic tests and electrochemical impedance spectroscopy (EIS) tests were performed at room temperature to study the corrosion behavior of the coating. The plate corrosion cell F029 (Tianjin Aida Hengsheng Technology Development Co., Ltd., Tianjin, China) was used to guarantee samples' exposure areas of 1 cm². The test solution was 3.5% sodium chloride solution to simulate the presence of Cl⁻ in seawater. The test was adopted in a standard three-electrode system by an electrochemical workstation of Inter-

face 1010E (Gamry, USA). The sample was the working electrode, saturated calomel electrode worked as reference electrode, and platinum mesh electrode was auxiliary electrode. Before the potentiodynamic tests and EIS tests, the open circuit potential (OCP) tests were conducted for 1 hour to get a stable state. The initial potential and the termination potential were set to -0.5 V and 0.5 V (relative to OCP), respectively. The scanning speed was 0.166 7 mV/s. When the corrosion potential remained stable, EIS tests were performed at a frequency of 100 kHz to 10 MHz by

0.01 V amplitude. Each value was obtained as the mean value of five measurements in a logarithmic sweep of frequencies. Impedance fitting was performed using Gamry Echem Analyst software.

1.3 Surface characterization

Scanning electron microscopy (EVO-18, Zeiss, Germany) was utilized to analyze the microstructure and surface morphology of the coating and its cross section. The porosity of the coating was calculated by image recognition method. Energy dispersive spectroscopy (EDS) analysis was performed to analyze the chemical compositions of the coating. In addition, X-ray diffractometer (D8 Advance, Bruker, Germany) with Cu-K α radiation was used to conduct X-ray diffraction (XRD). The scanning step distance was 0.04°, and the exposure time was 0.1 s/step.

2 Results and discussion

2.1 Structure of the coating

Fig. 1 presented SEM images of the surface and cross-section of HVOF Inconel 625 coating at different magnifications. Some unmolten and semi molten particles presented on the surface of the coating. Because the alloy powder was heated to the molten or semi molten state during spraying and this type of spraying powder, where molten liquid droplets and solid particles coexisted, solidified and accumulated after colliding with the substrate^[10]. The interface between the coating and the substrate was clear and well bonded, and no obvious voids and defects could be observed at interface. The coating was dense, without obvious cracks and defects. And there were a few voids. The coating thickness was uniform, with an average value of 520.41 μm in accordance with expectations. The porosity of the coating was about 0.21%, and the extremely low porosity was due to the extremely high kinetic energy during the deposition process leading to severe plastic deformation of molten particles^[12, 14].

Table 4 showed the EDS analysis of the coating surface. The results demonstrated that the chemical composition of the coating was consistent with that of Inconel 625 powder as expected. Besides, a small amount of oxygen was detected. Due to the oxidation of the powder during the spraying process, oxygen in the air was introduced into the coating, leading to a slight decrease in the proportion of alloy elements.

Fig. 2 represented the X-ray diffraction pattern (XRD) of HVOF Inconel 625 coating. The diffraction pattern proved that the Inconel 625 coating mainly presented Ni-Cr

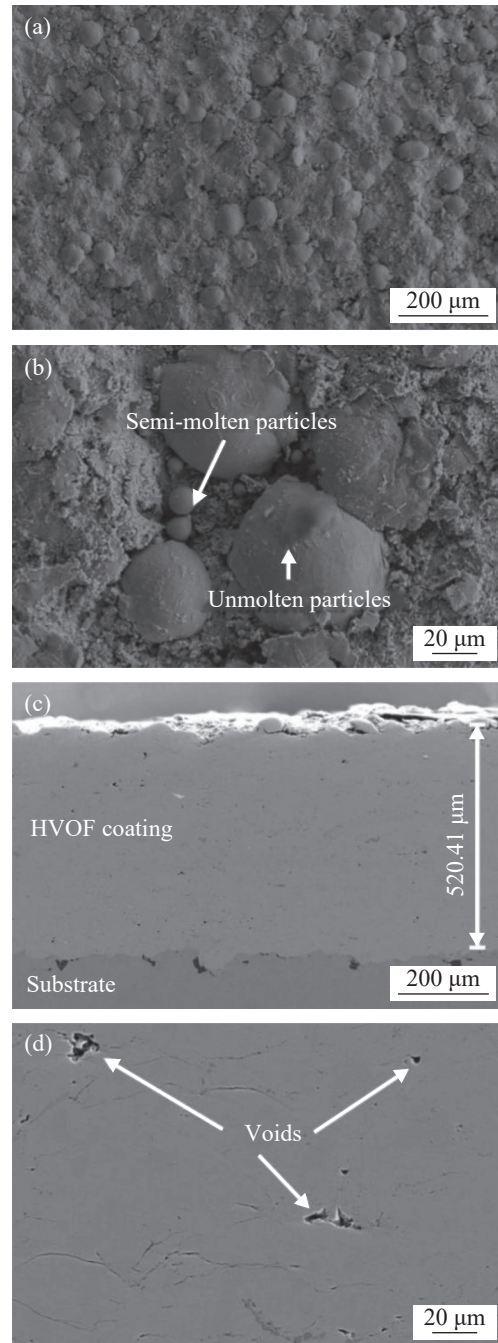
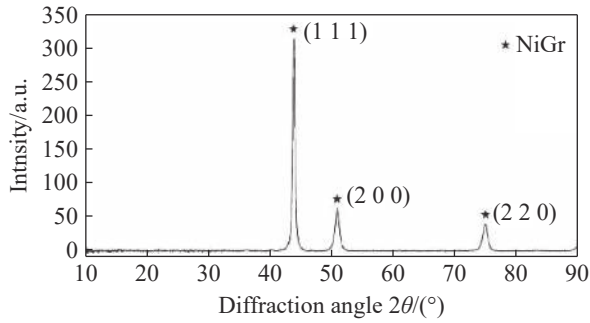


Fig. 1 SEM images of HVOF Inconel 625 coating before corrosion (a) Surface (100 ×), (b) Surface (500×) (c) Cross section (100×) (d) Cross section(500 ×)

phase with fcc structure(γ). The diffraction peak with the highest intensity at $2\theta = 41.69^\circ$ rationed to the (1 1 1) crystal plane. And peaks at around 2 theta = 50.75° and 73.76° corresponded to the (2 0 0) and the (2 2 0) crystal plane, respectively. As expressed earlier by Oladijo et al.^[8] and Chen et al.^[12], there was no oxide diffraction peak, which was consistent with previous EDS results.

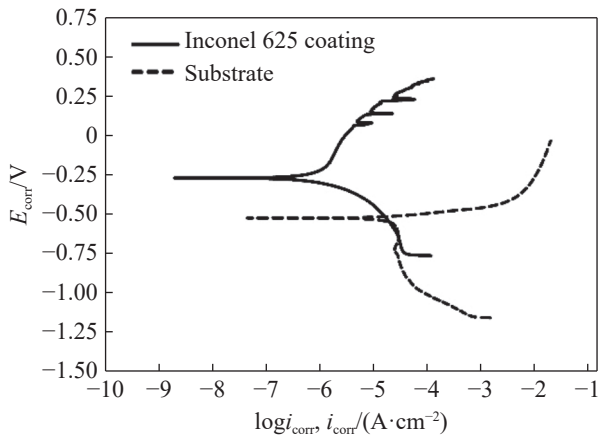
Table 4 Surface EDS results of HVOF Inconel 625 coating before corrosion (wt.%)

O	Si	Cr	Fe	Ni	Nb	Mo
4.54	1.09	20.81	2.46	61.89	2.48	6.72

**Fig. 2** XRD pattern of HVOF Inconel 625 coating

2.2 Electrochemical corrosion properties

The potentiodynamic polarization curve of HVOF Inconel 625 coating in 3.5% NaCl solution was shown in Fig. 3. The corrosion potential (E_{corr}) and corrosion current (i_{corr}) were listed in Table 5. The E_{corr} of the Inconel 625 coating was -272.0 mV and that of the Q235B substrate was -562.1 mV. The overall corrosion potential of the Inconel 625 coating displayed a notably positive trend. Its propensity to induce surface corrosion was relatively mild. And the corrosion resistance of the substrate was sig-

**Fig. 3** Potentiodynamic plots of HVOF Inconel 625 coating and reference samples**Table 5** Corrosion properties of HVOF Inconel 625 coating and reference samples

Sample	$E_{\text{corr}}/\text{mV}$	$i_{\text{corr}}/(10^{-6}\text{A}\cdot\text{cm}^{-2})$	Corrosion rate/(mm·year ⁻¹)
HVOF	-272.0	2.27	0.026 3
REF	-562.1	24.6	0.285

nificantly improved. The i_{corr} of the coating was 2.27×10^{-6} A/cm². Based on Faraday's law and ASTM G102-23^[15], the i_{corr} was converted to a self corrosion rate of about 0.026 3 mm/year. The i_{corr} of the substrate was 2.46×10^{-5} A/cm², corresponding to a self corrosion rate of approximately 0.285 mm/year after conversion. Compared with the corrosion rate of the substrate, the corrosion rate of the coating is one tenth that of the substrate. It indicated that HVOF Inconel 625 coating had excellent and stable corrosion resistance to Cl⁻^[11]. And the instability phenomenon observed in anodic region may be attributed by the microstructure of the coating, which comprised pores, cracks, splat boundaries, and regions with varying compositions^[16].

The Nyquist plots and the corresponding Bode plots of Inconel 625 coating in 3.5% NaCl solution were shown in Fig. 4. The Nyquist plot displayed the impedance data by the complex variables and separated into the real Z_{real} , and the imaginary Z_{im} , parts, expressed in $\Omega\cdot\text{cm}^2$. The EIS spectra of Inconel 625 coating exhibited a partially semicircle within Nyquist plot. The large semicircle of the capacitive arc always associated with the high polarization resistance. And the Bode plot displayed the frequency dependence of the absolute magnitudes of the impedance modulus, Z_{mod} , and the phase angle. Meanwhile, it displayed two time constant from Bode plot. In order to further analyze the corrosion process of Inconel 625 coating, an equivalent circuit was proposed to fit the EIS data shown in Fig. 5, and the EIS results for Inconel 625 coating were summarized in Table 6. R_s represented the electrolyte resistance. R_p was the resistance from the ionic conduction paths across the coating, and constant phase element-coating (CPE-c) represented the capacitance of the coatings. The parallel R_p -(CPE-c) group simulated the high-frequency semicircle, indicative of the open pores within the Inconel 625 coating being infiltrated by the electrolyte in anodic systems. CPE was a disturbed element used in place of a capacitor to compensate for non-homogeneity in the system, which was characterized by two parameters (Y and n). Y represented admittance constant(dielectric behavior or capacity) while n showed empirical exponent of CPE. Resistance R_t was the charge transfer resistance, and constant phase element-double-layer (CPE-d) represented the capacitance of the double layer^[17]. The parallel R_t -(CPE-d) group simulated the low-frequency semicircle, related to the electrolyte-electrode interface reaction. This reflected the anodic dissolution of the substrate^[18]. It has established that higher values of R_t and

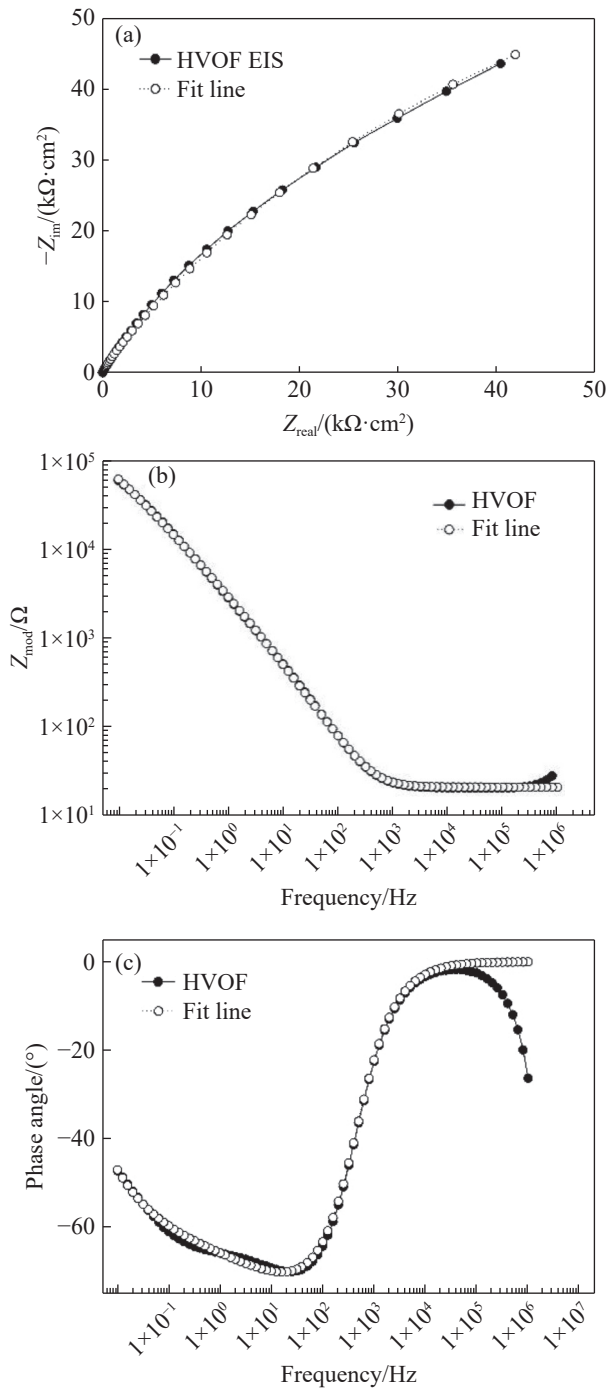


Fig. 4 Inconel 625 coating in 3.5% NaCl solution (a) Nyquist plot (b) Bode plot (c) Phase angle

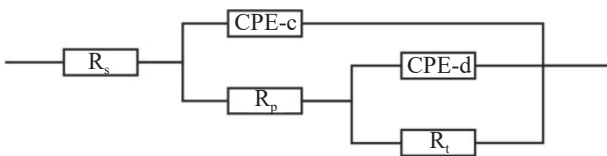


Fig. 5 Equivalent circuit model used for Inconel 625 coating

Table 6 EIS results of Inconel 625 coating after fitting with equivalent circuit

$R_s/$ ($\Omega \cdot \text{cm}^{-2}$)	$R_p/$ ($\Omega \cdot \text{cm}^{-2}$)	$R_t/$ ($10^3 \Omega \cdot \text{cm}^{-2}$)	$Y_c/(10^{-6} \Omega^{-1} \cdot \text{cm}^{-2} \cdot \text{S}^{-n})$		n	
			CPE-c	CPE-d	CPE-c	CPE-d
20.98	3.322	222.9	14.29	78.92	1.000	0.656

lower values of CPE-c indicated improved corrosion protection capabilities of the coatings. Additionally, the lower CPE-c values correlated with reduced porosity of the coating, which was consistent with the conclusions from the previous chapter^[19].

3 Conclusions

(1) The Inconel 625 coating with dense microstructure and low porosity was obtained by HVOF, and the coating bonded well to the substrate without cracks.

(2) Based on potentiodynamic polarization tests, the corrosion rate of the coating under the condition of 3.5% NaCl solution at room temperature was 0.026 3 mm/year, which was one tenth of that of the substrate. It illustrated that HVOF Inconel 625 layer presented high resistance for the presence of Cl^- .

(3) EIS spectra demonstrated that the Inconel 625 coating presented excellent corrosion protection ability and low porosity.

References

- [1] Procópio L. The role of biofilms in the corrosion of steel in marine environments. *World Journal of Microbiology and Biotechnology*, 2019, 35(5):73.
- [2] Pradhan D, Mahobia G S, Chattopadhyay K, et al. Effect of surface roughness on corrosion behavior of the superalloy IN718 in simulated marine environment. *Journal of Alloys and Compounds*, 2018, 740:250 – 263.
- [3] Tian Y, Zhang H, Chen X, et al. Effect of cavitation on corrosion behavior of HVOF-sprayed WC-10Co4Cr coating with post-sealing in artificial seawater. *Surface & Coatings Technology*, 2020, 397:126012.
- [4] Brijpal S. Influence of flux composition on microstructure and oxygen content of low carbon steel weldments in submerged arc welding. *China Welding*, 2018, 27(1): 10 – 19.
- [5] Zhou Y J, Deng D A, Liu X Z, et al. Influences of external restraint on welding distortion in low carbon steel bead-on thin plate joints. *China Welding*, 2017, 26(1):9 – 14.
- [6] Song B, Voisey K T, Hussain T. High temperature chlorine-induced corrosion of Ni50Cr coating: HVOF, HVOGF, cold spray and laser cladding. *Surface & Coatings*

- [Technology](#), 2018, 337:357 – 369.
- [7] Szymański K, Hernas A, Moskal G, et al. Thermally sprayed coatings resistant to erosion and corrosion for power plant boilers-A review. [Surface & Coatings Technology](#), 2015, 268:153 – 164.
- [8] Oladijo O P, Luzin V, Maledi N B, et al. Residual stress and wear resistance of HVOF Inconel 625 coating on SS304 steel substrate. [Journal of Thermal Spray Technology](#), 2020, 29:1382 – 1395.
- [9] Liu H D, Wang W Q, Liu Y. Failure analysis of a bellows expansion joint of Inconel625 alloy. [Advanced Materials Research](#), 2012, 500:580 – 585.
- [10] Li Y, Liang T, Ao R, et al. Oxidation resistance of iron-based coatings by supersonic arc spraying at high temperature. [Surface and Coatings Technology](#), 2018, 347:99 – 112.
- [11] Yung T Y, Chen T C, Lu W F, et al. Thermal spray coatings of Al, ZnAl and Inconel 625 alloys on SS304L for anti-saline corrosion. [Coatings](#), 2019, 9(32):1 – 12.
- [12] Chen T C, Chou C C, Yung T Y, et al. A comparative study on the tribological behavior of various thermally sprayed Inconel 625 coatings in a saline solution and deionized water. [Surface & Coatings Technology](#), 2020, 385:125442.
- [13] Yang E J, Li T J, Li W, et al. Thermal corrosion resistance of Ni-based coating prepared by HVOF/HVAF. [Heat Treatment of Metals](#), 2018, 43(7):209 – 214.
- [14] Illana A, de Miguel M T, García-Martín G, et al. Experimental study on steam oxidation resistance at 600 °C of Inconel 625 coatings deposited by HVOF and laser cladding. [Surface & Coatings Technology](#), 2022, 451:129081.
- [15] ASTM International. Standard practice for calculation of corrosion rates and related information from electrochemical measurements: ASTM G102-23. West Conshohocken, United States, 2023:1 – 7.
- [16] Niaz A, Bakare M S. Electrochemical corrosion testing and characterization of potential assisted passive layer on HVOF Inconel 625 coating. [Corrosion Reviews](#), 2015, 33(1 – 2): 63 – 76.
- [17] Kang Y, Chen Y, Wen Y, et al. Effects of structural relaxation and crystallization on the corrosion resistance of an Fe-based amorphous coating. [Journal of Non-Crystalline Solids](#), 2020, 550:120378.
- [18] Hong S, Wei Z, Wang K, et al. The optimization of microbial influenced corrosion resistance of HVOF sprayed nanostructured WC-10Co-4Cr coatings by ultrasound-assisted sealing. [Ultrasonics Sonochemistry](#), 2021, 72:105438.
- [19] Jiang J, Wang Y, Zhong Q, et al. Preparation of Fe₂B boride coating on low-carbon steel surfaces and its evaluation of hardness and corrosion resistance. [Surface & Coatings Technology](#), 2011, 206(2 – 3):473 – 478.